Application of new Eurocode 3 formulae for beam-columns to Class 3 hollow section members

N. Boissonnade & K. Weynand
Feldmann + Weynand GmbH, Aachen, Germany

J.P. Jaspart
ArGEnCo Department, University of Liège, Liège, Belgium

ABSTRACT: This paper presents a new set of design formulae for Class 3 hollow section beam-column members. The specificity of the proposed rules consists in offering a fully continuous model along the Class 3 range, filling the existing gap between plastic and elastic resistance in Eurocode 3. Through comparisons with both experimental tests and extensive FEM numerical results, the proposal is found accurate and safe. Moreover, a second parametric study dedicated to the determination of the level of safety led to a fully satisfactory safety factor γ_M.

1 INTRODUCTION

This paper reports on investigations led towards the application of the new Eurocode 3 formulae for hollow section beam-columns. More precisely, it (i) focuses on the behavior of semi-compact "Class 3" cross-section members, and (ii) presents the essentials of a new design model for the resistance of Class 3 cross-sections.

The new set of design rules for checking the stability of beam-column members proposed in the latest version of Eurocode 3 (EN 1993–1–1 2005) differ significantly from the previous ENV version set (ENV 1993–1–1 1992). Two different sets of formulae are now available, according to either Method 1 or Method 2. Based on second-order principles, both methods provide a high level of accuracy and emphasize a clear physical background, which is of prime importance for a safe day-by-day application.

Besides this, recent research efforts on the behavior and design of Class 3 cross-sections have been undertaken, within RFCS research project "Semi-Comp". The outcome of the project mainly consisted in an improved analytical formulation for cross-section resistance that enables a fully continuous transition between the *plastic* bending resistance $M_{pl,Rd}$ at the Class 2 – 3 border and the *elastic* bending resistance $M_{el,Rd}$ at the Class 3 – 4 border: indeed, as Figure 1 shows, such a gap still exists in Eurocode 3, associated with the principles of cross-section classification. Present paper shows how this new concept for semi-compact cross-sections can be successfully incorporated in the more general context of beam-column members with Class 3 cross-sections.

In a first step, the paper proposes a brief review of the new beam-column formulae with a particular emphasis on their main features; then, the basic principles of the proposed Class 3 cross-section resistance model are detailed in Section 2. Section 3 focuses on the validation of a purposely-derived FEM tool towards experimental tests; this numerical tool is extensively used in the parametric studies described in Section 4, where comparisons with the results provided by the design formulae are presented.

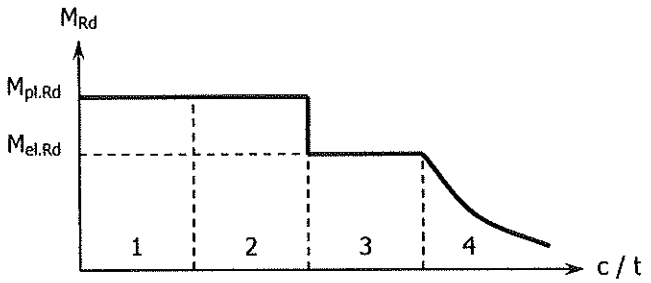

Figure 1. Distribution of bending resistance along cross-section class ranges according to Eurocode 3.

2 NEW DESIGN FORMULAE FOR CLASS 3 HOLLOW SECTION MEMBERS

2.1 *New beam-column formulae in Eurocode 3*

As already mentioned, the new beam-column rules in Eurocode 3 consist in two different sets, Method 1 and 2, given separately in Annexes A and B, respectively (each country has the possibility to recommend one of the formulae set, by means of the National Annexes).

Method 1 has been basically built on the principles of generality, consistency and continuity with the

other formulae of the code; it provides a high level of accuracy, and is applicable to any type of cross-section. Reference is especially made here to Method 1 set of design rules that have been derived in order to fulfill the following requirements: accuracy, generality, consistency, continuity, transparency and mechanical basis (Boissonnade et al. 2006, CIDECT 2007).

Method 2 is dedicated to a more simple and practical use, through global factors that cover several physical effects; specific formulae for hollow cross-sections are also proposed.

The basic format of both methods relies on elastic second-order considerations. Spatial behavior and elastic-plastic behavior have been progressively incorporated in the elastic in-plane format (Boissonnade et al. 2006), and the general formulae for Method 1, rearranged in a suitable format, are as follows (for Class 1 and 2 cross-sections):

$$\frac{N_{Ed}}{\chi_y N_{pl,Rd}} + \mu_y \left[\frac{C_{my} M_{z,Ed}}{\left(1 - N_{Ed}/N_{cr,y}\right) C_{yy} M_{pl,y,Rd}} \right] + \gamma^* \mu_y \left[\frac{C_{mz} M_{z,Ed}}{\left(1 - N_{Ed}/N_{cr,z}\right) C_{yz} M_{pl,z,Rd}} \right] \le 1 \quad (1)$$

$$\frac{N_{Ed}}{\chi_z N_{pl,Rd}} + \delta^* \mu_z \left[\frac{C_{my} M_{z,Ed}}{\left(1 - N_{Ed}/N_{cr,y}\right) C_{zy} M_{pl,y,Rd}} \right] + \mu_z \left[\frac{C_{mz} M_{z,Ed}}{\left(1 - N_{Ed}/N_{cr,z}\right) C_{zz} M_{pl,z,Rd}} \right] \le 1 \quad (2)$$

As can be seen, the formulae presented here make use of the well-known amplification factor concept. Also, the concept of equivalent moment factor C_m is employed; it can be shown that the definitions of oth of them are intrinsically dependent on each other (Boissonnade et al. 2006).

The use of an equivalent moment factor is a first important feature of the proposed formulae. It brings significant simplification since it allows substituting the (general) actual bending moment distribution on the member for an equivalent one that leads to the same maximum second-order bending moment on the member M^{max}, see Figure 2.

In the particular case of a linear bending moment, which is of prime importance in practice, Method 1 proposes a new expression for C_m:

$$C_m = 0.79 + 0.21\psi + 0.36\left(\psi - 0.33\right)\frac{N_{Ed}}{N_{cr}} \quad (3)$$

where ψ is the ratio between the applied end moments ($-1 \le \psi \le 1$). This last definition, when compared to well-know definitions such as the ones of Austin (Austin 1981) or Massonnet (Massonnet & Campus 1955), significantly improves the accuracy of the beam-column formulae, where the determination of C_m is decisive.

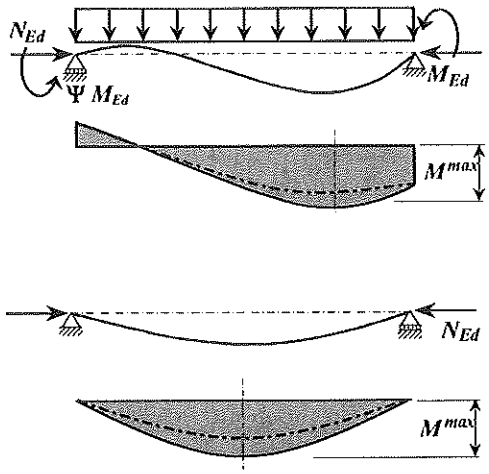

Figure 2. Illustration of equivalent moment factor C_m concept.

Besides this, Method 1 proposes to take due account of elastic-plastic effects by means of (i) C_{ii} and C_{ij} factors for $M-N$ interactions (i and j indexes are relative to either $y-y$ or $z-z$ axes, see Eq. (4)) and (ii) γ^* and δ^* factors for $M_{y,Ed} - M_{z,Ed}$ biaxial bending interaction.

Since instability effects influence the extent of yielding in the member, the plastic cross-section resistance $M_{pl,Rd}$ of a Class 1 or 2 section might not be reached, but an elastic-plastic $C\,M_{pl,Rd}$ one, where C is so that $C\,M_{pl,Rd}$ is comprised between $M_{pl,Rd}$ and $M_{el,Rd}$. When spatial behavior and loading must be contemplated, a distinction has to be made between what concerns strong axis and weak axis, therefore the need to introduce distinctive C_{ii} and C_{ij} coefficients (Boissonnade et al. 2006). The general writing of the C_{ii} factor is as follows:

$$C_{ii} = 1 + \left(w_i - 1\right)\left[2 - \frac{1.6}{w_i} C_{mi}^{\,2} \left(\bar{\lambda}_i + \bar{\lambda}_i^{\,2}\right)\right] \frac{N_{Ed}}{N_{pl,Rd}} \ge \frac{W_{el,i}}{W_{pl,i}} \quad (4)$$

with $w_i = W_{pl,i} / W_{el,i} \le 1.5$. W_{pl} and W_{el} designate respectively the plastic and elastic modulus of the member cross-section in bending; $\bar{\lambda}_i$ represents the relative column slenderness for flexural instability.

The definition of C_{ii} must obviously depend on $\bar{\lambda}_i$, so that the behavior of the beam is plastic for small slenderness, and becomes elastic as the member slenderness and the axial compression increase. In Eq. (4), the factor $(w-1)$ represents the maximum available bending potential between pure elasticity and pure plasticity, and must be multiplied not only by a function of $\bar{\lambda}_i$, as explained before, but also by a function of C_m, because the member cannot develop the same elastic-plastic effects whatever the transverse loading is. This calibrated coefficient then clearly permits a smooth physical transition between plasticity and elasticity; the bending moment of the column cross-sections being always greater than the elastic moment resistance, the C_{ii} coefficient must be

bounded by W_{el}/W_{pl} for Class 1 and 2 cross-sections.

As explained before, γ^* and δ^* are factors to account for biaxial bending elastic-plastic interaction; they are respectively chosen as $0.6\sqrt{w_z/w_y}$ and $0.6\sqrt{w_y/w_z}$.

As one of the most outstanding features of the Method 1 set of design formulae, *continuity aspects* have been receiving specific attention. It can be observed that the different formulae provide continuity:

- from elastic to plastic behavior;
- from cross-section to member resistance when the member slenderness increases:
- with the other formulae of the code;
- between simple loading situations;
- from spatial to in-plane behavior.

Finally, it has to be mentioned that the proposed formulae have been validated for Class 1 and 2 cross-section members (both open and hollow section shapes) on about 15 000 non-linear GMNIA FEM simulations results as well as on 370 test results (Boissonnade et al. 2006, CIDECT 2007).

2.2 *Proposal for a design model for Class 3 hollow section members*

As Eqs. (1) and (2) show, the new beam-column formulae have been mainly built for *plastic* Class 1 and 2 cross-sections. However, Class 3 and 4 cross-sections situations are obviously covered, since the basis of the formulae is *elastic* behavior (Boissonnade et al. 2006).

As already mentioned, the formulae have been derived so that to offer a maximum level of continuity; nevertheless, a lack of continuity in bending resistance can be observed at the Class 3 to 4 border, as Figure 1 shows. Indeed, in accordance with Eurocode 3 assumptions, the cross-section resistance for pure bending drops from $M_{pl,Rd}$ to $M_{el,Rd}$ when the cross-section passes from Class 2 to Class 3. More than 50% of resistance may be lost due to the presence of this gap, which is physically not acceptable; the loss of resistance may rise up to 65% when biaxial bending is of concern.

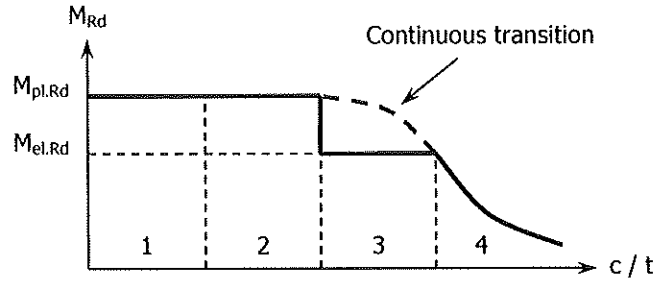

Figure 3. Proposed continuous distribution of bending resistance along cross-section class ranges.

In order to propose a solution to this problem, a RFCS research project named "Semi-Comp" has been initiated, where a mechanical model for a continuous cross-section and member buckling resistance along the Class 3 field has been developed. The basic idea on which the model relies on consists in offering an intermediate "elastic-plastic" resistance of the semi-compact cross-section in bending, between pure plastic and pure elastic behavior (see Figure 3). In this way, the distribution of stresses of Figure 4 is adopted. The total bending resistance then consists of two distinctive contributions (Eq. (5)):

- a plastic contribution $W_{3,pl}f_y$ that corresponds to the yielded fibers of the section;
- an elastic contribution $W_{3,el}f_y$ arising from the other fibers of the section that have not reached the yield stress (fibers within h_{ep}, see Figure 4).

$$M_{3,Rd} = \left(W_{3,pl} + W_{3,el}\right) f_y \tag{5}$$

Obviously, the key aspect here lies in the correct determination of h_{ep}, that must be so that the cross-section reaches a full plastic resistance at the Class 2 – 3 border (i.e. $h_{ep} \to 0$), and that the cross-section exhibits its sole elastic resistance at the Class 3 – 4 border (i.e. $h_{ep} = h$).

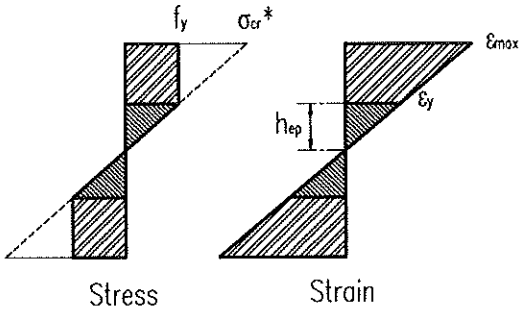

Figure 4. Elastic-plastic distribution of stresses.

This is achieved in assuming that whenever the stress distribution were still linear beyond f_y, the maximum stress reached would be equal to σ_{cr}, at a strain level $\varepsilon = \varepsilon_{max} > \varepsilon_y$, ε_y being the maximum elastic strain. The critical plate stress σ_{cr} appears as a convenient stress measure here, since the local (plate) instability effects play the key role here.

$$\sigma_{cr} = \frac{k_\sigma \pi^2 E}{12\left(1-\nu^2\right)}\left(\frac{t}{b}\right)^2 \tag{6}$$

However, in order to fulfill the continuity aspects at the ends of the Class 3 field, it is necessary to bring modifications to the original definition of σ_{cr}. Indeed in accordance with Figure 4, σ_{cr} must be so that:

- $\sigma_{cr} = \infty$ at the limit between Class 2 and Class 3;
- $\sigma_{cr} = f_y$ at the limit between Class 3 and Class 4.

In the particular case of a simply supported plate in compression, such a modified σ_{cr}^* writes:

$$\sigma_{cr}^* = 1.616\,E\left(\frac{1}{9.5c/t - 323\varepsilon}\right)^2 \tag{7}$$

It is to be noted that this definition stands for a Class 3 field defined for so-called c/t ratios comprised between 34ε and 38ε, unlike the 38ε to 42ε one prescribed by Eurocode 3. Place is missing here to provide full justifications for this fact (cf. Semi-Comp 2007).

Finally, the design model resorts to the plastic cross-section design checks of Eurocode 3 for combined loading, adequately modified to allow for continuous transitions along the Class 3 range:

$$M_{N,3,y,Rd} = M_{3,y,Rd}\frac{1-n}{1-0.5a\left(1-\frac{f_y}{\sigma_{cr}^*}\right)} \le M_{3,y,Rd} \quad (8)$$

$$M_{N,3,z,Rd} = M_{3,z,Rd}\frac{1-n}{1-0.5a\left(1-\frac{f_y}{\sigma_{cr}^*}\right)} \le M_{3,z,Rd} \quad (9)$$

$$\left(\frac{M_{y,Ed}}{M_{N,3,y,Rd}}\right)^{\alpha^*} + \left(\frac{M_{z,Ed}}{M_{N,3,z,Rd}}\right)^{\beta^*} \le 1 \quad (10)$$

$$\text{where } \alpha^* = \beta^* = \frac{1.66}{1-1.13n^2}\left(1-\frac{f_y}{\sigma_{cr}^*}\right) + \frac{f_y}{\sigma_{cr}^*} \le 6 \quad (11)$$

These equations ensure full continuity with the simple loading cases and within the Class 3 range.

The implementation of this cross-section model is straightforward in the Method 1 set of *beam-column* design formulae. Obviously, one must replace $M_{pl,y,Rd}$ and $M_{pl,z,Rd}$ by $M_{3,y,Rd}$ and $M_{3,z,Rd}$ in the different factors, such as for w_y and w_z in the C_{ij} factors for example. In addition, the γ^* and δ^* factors need to be adjusted to:

$$\gamma^* = 0.6\sqrt{\frac{w_z}{w_y}}\left(1+\frac{1-0.6\sqrt{\frac{w_z}{w_y}}}{0.6\sqrt{\frac{w_z}{w_y}}}\frac{f_y}{\sigma_{cr}^*}\right) \quad (12)$$

$$\delta^* = 0.6\sqrt{\frac{w_y}{w_z}}\left(1+\frac{1-0.6\sqrt{\frac{w_y}{w_z}}}{0.6\sqrt{\frac{w_y}{w_z}}}\frac{f_y}{\sigma_{cr}^*}\right) \quad (13)$$

3 ASSESSMENT OF FEM NUMERICAL TOOLS

3.1 *Tests on Class 3 hollow section members*

Within the frame of "Semi-Comp" project, a series of 24 tests on beam-column members has been undertaken. The main goal of the tests was to help validating a purposely-derived FEM model that, if found satisfactory, would be used extensively in parametric studies (see section 4).

Amongst the 24 member buckling tests, 6 were performed on RHS 200x120x4 (S275) members, and 6 on SHS 180x5 (S355) members; all profiles were about 4000 *mm* long.

In order to fully characterize the different specimens, in view of further comparison with the FEM calculations, several additional measurements and tests have been conducted, mainly regarding dimensions, material characteristics and initial imperfections.

Accordingly, several tensile coupon tests have been completed, including in the corner regions, to provide the necessary information on material behavior (see Table 1).

Table 1. Results for tensile coupon tests.

	E	f_y	f_u
Section	*GPa*	N/mm^2	N/mm^2
RHS 200x120x4 (S275)	177	378	486
SHS 180x5 (S355)	178	413	538

The coupon tests first showed that the $\sigma-\varepsilon$ curves were not exhibiting a typical "yield plateau", as is usual for constructional steel; consequently, a specific implementation has been made in the FEM models, and the determination of the design yield stress has been made possible through the "$f_{y\,0.2\%}$ procedure".

Secondly, these tests revealed, as expected, a much higher level of yield stress in the corner zones, due to strain hardening (resp. 548 N/mm^2 for RHS cross-sections and 520 N/mm^2 for SHS sections).

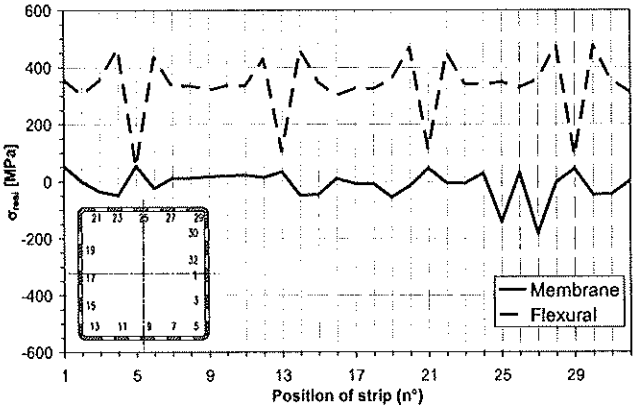

Figure 5. Measured initial residual stresses on SHS180x5 section.

Besides this, the so-called "cutting strip technique" was used for the determination of initial residual stresses. This method consists in measuring the length of several strips all over the cross-section (see Figure 5) before and after cutting of the strips. The differences in length are directly linked to membrane stresses, while additional measurements of the

variation of curvature provide further information on the flexural initial residual stresses.

Figure 5 presents some of the obtained results, where a rather low level of initial membrane residual stresses is observed, in comparison with the level of initial flexural residual stresses, as was expected.

Information on the initial geometrical imperfections is also decisive for the correct interpretation of member buckling tests: it is indeed known to have a non negligible influence on the carrying capacity of real members. In the present project, it was necessary to determine both the "global" longitudinal imperfections and the "local" (plate) defaults, since the occurrence of local buckling is a key feature in the behavior of Class 3 cross-section members.

Accordingly, imperfections on several faces of the tested members have been measured all along the specimens' length, at three different points in a cross-section (see Figure 6).

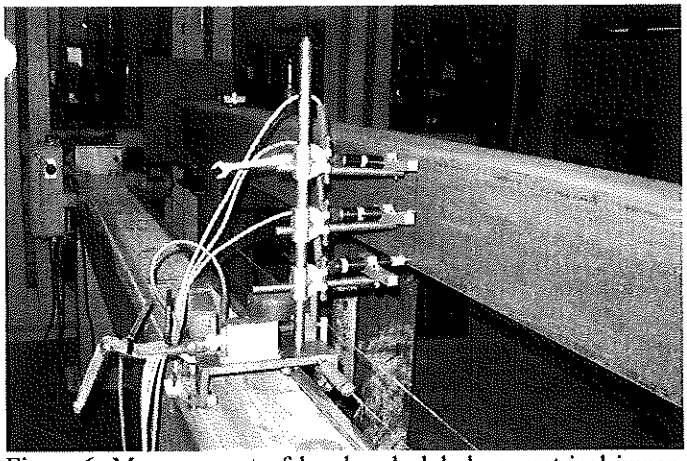

Figure 6. Measurement of local and global geometrical imperfections on a face.

Three measurement devices have then been fixed on a small trolley that displaces all along the specimen's length, recording the longitudinal defaults along three different lines. Through appropriate geometrical treatment, it becomes possible to separate the member *global* imperfection from the *local* imperfection. Indeed, a measurement close to the corner zone of a tubular profile is assumed to be free from local imperfections, i.e. representative of the global imperfection, while a measurement in the middle of a face contains both local and global defaults. Figure 7 shows an example of result where global and local imperfections have been separated.

It was finally found that the relative level of both global and local initial imperfections was small, though highly variable from one specimen to another. These data (shape and amplitude) have been further implemented in the FEM models for validation purposes.

The member buckling main tests consisted in monaxial or biaxial bending with axial compression tests. For convenient purposes, primary bending was applied through eccentrically applied thrust. As a consequence, the primary bending moment diagrams applied on the members were linear (with $\psi = 1$ or $\psi = 0$ values).

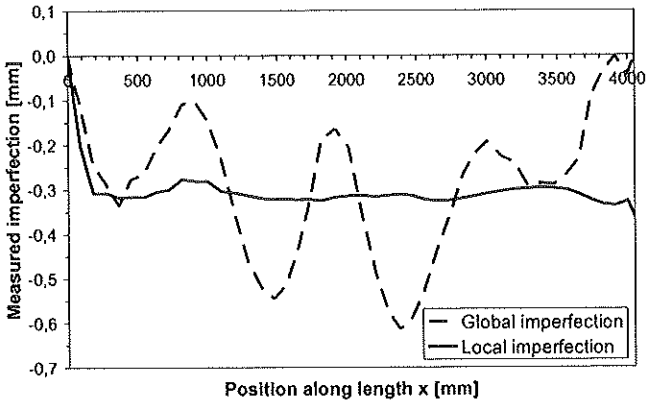

Figure 7. Geometrical global and local imperfections (RHS 180x5 profile, strong axis).

The support conditions of the members during the tests may be assumed to be "pinned conditions": the end-sections bending rotations can be assumed to be free, since the specimen was fixed at its bottom and top to half-spheres lying on a film of oil ensuring a low level of friction; the centre of these half-spheres were exactly located at the member's end sections; torsional rotation of the member ends was also prevented. So-called end plates were also welded to the specimens end sections, so that to fix them in the test rig. Axial compression was applied through controlling the pressure of oil in the system.

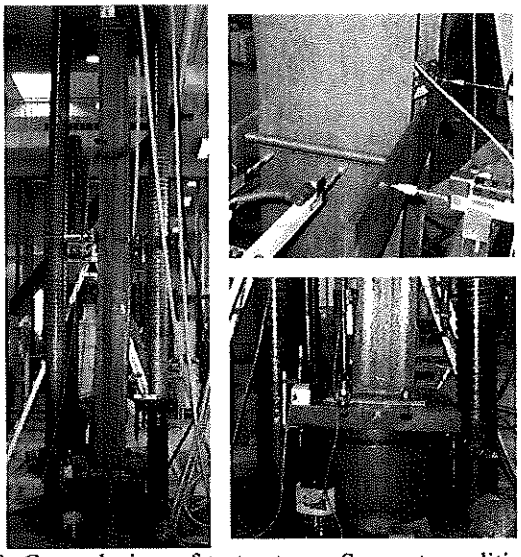

Figure 8. General view of test setup – Support conditions and instrumentation in the mid-height cross-section and at supports.

For each test, the following data have been recorded: applied load, axial shortening, and at top and bottom of the specimens, rotations in both principal planes. For the mid-span cross-section, major and minor axis displacements were measured. This information has been further used in comparisons with the FEM results.

3.2 *Comparison with FEM models and design proposal*

Adequate FEM numerical models (see Figure 9) have been developed, that resorts to *shell* elements: indeed, the key aspect here consists in characterizing the early or late occurrence of *local buckling* on the behavior of the semi-compact cross-section member, thus the need for shell elements.

Specific attention has been paid to the meshing of the corner regions, and mesh-density tests have been performed for each possible type of analysis.

Additional fictitious nodes have been defined at the centroids of the end cross-sections for the definition of the support conditions.

Realistic boundary conditions (i.e. with welded plates at the ends of the members) as well as measured characteristics (material law, dimensions, and geometrical imperfections) have been introduced in the numerical models, in order to perform a comparison with the experimental tests as accurate as possible.

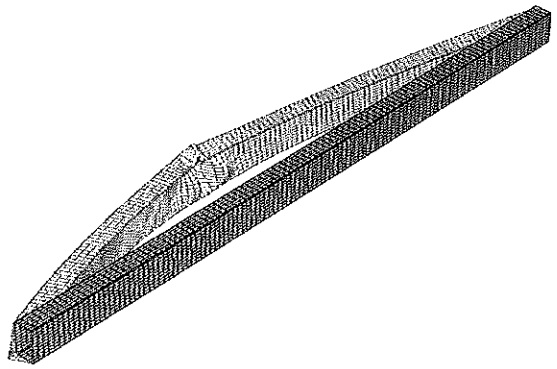

Figure 9. Shell FEM model (amplified deformation at failure and initial shape).

It is to be noted that no initial residual stresses have been introduced in the numerical models, since they mainly consist in *flexural* residual stresses (see section 3.1) that are know to have a lesser influence than the *membrane* residual stresses which are negligible here.

Table 2 presents the results obtained for both RHS and SHS test series.

Table 2. Results for hollow section member buckling tests.

Specimen	e_y [mm]	e_z [mm]	P_{test} [kN]	P_{FEM} [kN]	P_{model} [kN]	$\%_{FEM}$	$\%_{model}$
R275_BU_1 ($\psi = 1$)	55	0	404	378	294	7.0	37.2
R275_BU_2 ($\psi = 0$)	55	0	451	453	331	-0.4	36.3
R275_BU_3 ($\psi = 1$)	0	45	261	239	211	9.2	23.9
R275_BU_4 ($\psi = 0$)	0	45	331	296	240	12.0	38.1
R275_BU_5 ($\psi = 1$)	55	45	268	225	183	19.3	46.7
R275_BU_6 ($\psi = 0$)	55	45	307	282	217	8.8	41.5
S355_BU_1 ($\psi = 1$)	55	0	563	546	449	3.1	25.4
S355_BU_2 ($\psi = 0$)	55	0	656	660	509	-0.6	29.0
S355_BU_3 ($\psi = -0.45$)	55	0	708	700	532	1.2	33.1
S355_BU_4 ($\psi = 1$)	55	55	460	453	328	1.6	40.3
S355_BU_5 ($\psi = 0$)	55	55	600	568	382	5.5	57.1
S355_BU_6 ($\psi = -0.45$)	55	55	629	608	419	3.4	50.0

In addition to the experimental maximum axial loads, Table 2 reports the results of the FEM calculations and the analytical results yielded by the application of the model described in section 2.2. It also provides information on the applied loading: monoaxial or biaxial bending, and constant ($\psi = 1$) or triangular ($\psi = 0$) first order bending moment.

First, a very good agreement between experimental and numerical results can be observed: the difference is usually less than 5% (except for two results where the experimental load exceeds the FEM load by about 20%), and is always on the safe side.

Considering the uncertainties inherent to the experimental setup and material behavior, the results presented herein are assumed to be satisfactory enough to validate the ability of the FEM models to simulate the behavior of such Class 3 cross-section members up to collapse. Accordingly, the developed FEM models have been intensively used in parametric studies, as detailed in the next section.

Besides this, Table 2 also shows rather conservative results obtained through the application of the proposed model. This can first be explained by the difference between the assumed levels of imperfections: indeed, the design model implicitly accounts for a rather high level of imperfections, while the measured one was relatively small, which leads to over-conservative design results.

Secondly, due to the delivery of test specimens exhibiting a higher yield stress than expected (see Table 1), all cross-sections are classified as Class 4 sections. As a consequence, a reduced (effective) analytical resistance can only be reached, while the members exhibited a certain amount of elastic-plastic effects, therefore the high level of safety of the design formulae.

4 PARAMETRIC STUDIES

The numerical models being shown to be accurate and appropriate, extensive parametric studies have been performed. The following parameters have been taken into account in a first parametric study:

- 2 different cross-section shapes: RHS 250x150x6 and SHS 180x5;
- 2 different steel grades: $f_y = 235\ N/mm^2$ and $f_y = 355\ N/mm^2$;
- 2 primary linear bending moments distributions: $\psi_y = \psi_z = 1$ and $\psi_y = \psi_z = 0$ ($M_{y,Ed}$ and $M_{z,Ed}$ end-moments applied on the same side);
- 2 relative slenderness $\lambda_z = 0.5$ and $\lambda_z = 1.0$;
- 4 different values of relative axial compression $n = N_{Ed} / N_{b,Rd}$: $n = 0$, 0.30, 0.50 and 0.70, where $N_{b,Rd}$ represents the flexural buckling load under pure compression;
- For each fixed values of the previous parameters, 9 combinations of $M_{y,Ed}$ and $M_{z,Ed}$ values have

been investigated, so that to allow for the determination of the biaxial bending interaction.

Steel grade S355 have been studied as it has now become the "standard" one, and S235 was also kept in the calculations in order to exhibit a more plastic behavior. Indeed, the influence of instability phenomena (i.e. local buckling) is more pronounced for high strength steel, and as a consequence, the expected elastic-plastic behavior of Class 3 member may be more pronounced for S235 than for S355 steel. In the same way, the relative low values of λ_z have been chosen so as the buckling behavior of members to be influenced by elastic-plastic effects, since the influence of member instabilities (i.e. flexural buckling or lateral torsional buckling) makes the behavior of members nearly elastic for high relative member slenderness ($\lambda > 1.0$).

For each plate of the different cross-sections, a *local* geometrical imperfection has been accounted for, along the clear width of the considered plate. It consists in a doubly sinusoidal shape (i.e. in both longitudinal and transversal directions) with maximum amplitude equal to $b / 200$, b being the clear width.

In addition, a *global* imperfection has been introduced, that consists in a combination of sinusoidal out-of-straightness for both strong and weak axis (maximum amplitude $L / 1000$ at mid-span). Considering such a level of initial geometrical imperfection in both principal axes together with the adopted local one appears to be rather severe, and should therefore lead to safe results.

The values of axial buckling loads $N_{b,Rd}$ have been obtained through separate calculations. The level of relative axial compression n has been applied trough a first load sequence where N_{Ed} applies until the expected level; a second load sequence followed where N_{Ed} is fixed and both $M_{y,Ed}$ and $M_{z,Ed}$ were rising simultaneously. Doing so affects the expansion of second-order effects, since the coupling between lateral displacements caused by primary bending and the axial force may not be the same as in a situation where all the internal (1st order) forces rise proportionally.

In total, 576 non-linear FEM-shell calculations have been performed.

Besides these FEM simulations, their equivalent analytical counterparts have been calculated, in order to investigate the accuracy of the proposed model for Class 3 members. It is to be noted that the results presented herein do not allow for a rigorous determination of the benefits brought by either the semi-compact cross-section model or the new beam-column formulae, since the global response of the *member* is studied here. However, within the frame of the Semi-Comp project, the cross-section model has been shown accurate and safe through other specific parametric studies (Semi-Comp 2007), while the new beam-column formulae have been deeply investigated and validated, cf. section 2.1 (Boissonnade et al. 2006).

Table 3. Results for accuracy parametric study.

	RHS 200x120x4		SHS 180x5	
	$\psi = 1$	$\psi = 0$	$\psi = 1$	$\psi = 0$
m	1.263	1.316	1.275	1.340
s	0.141	0.183	0.229	0.307
min	0.916	0.907	0.903	0.917
max	1.552	1.756	1.820	2.092
< 0.97	4	7	7	15
Σ tests	144	144	144	144
Σ Class 4	22	22	16	16

Table 3 proposes a summary of results on the comparison between numerical and analytical results. The values reported refer to so-called R_{simul} values, which represent the ratio of the $M_{y,Ed} - M_{z,Ed}$ loading leading to failure according to the FEM result to the *proportional* $M_{y,Ed} - M_{z,Ed}$ loading leading to failure according to the proposed formulae. Consequently, a value higher than unity means safety, while a value lower than one indicates an unsafe result. The R_{simul} values also form a good indicator of the level of accuracy of the proposal: a value of 1.10 indicates a 10% resistance reserve.

As can be seen in Table 3, the mean m and standard deviation s values of the R_{simul} ratios are quite satisfactory, highlighting the good accuracy of the proposal. Table 3 indicates in addition minimum and maximum values of R_{simul}, together with an $R_{simul} < 0.97$ criterion that intends at collecting the "real" unsafe situations, i.e. that cannot be charged to the interaction formulae (it is known that Eurocode 3 recommendations for flexural buckling can be up to 3% on the unsafe side compared to FEM results, thus the 0.97 value).

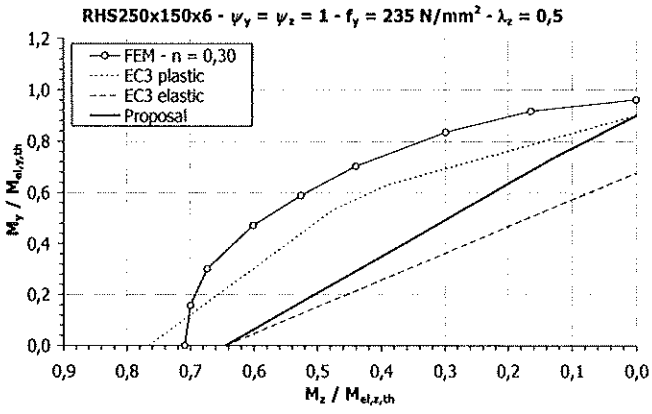

Figure 10. Illustration of an intermediate behavior.

Figure 10 also further illustrates the ability of the proposed model to lead to intermediate results between full plastic behavior and pure elastic behavior. It also clearly shows that in this particular case, it would appear unnecessarily conservative to restrict the resistance of such members to their sole *elastic* carrying capacity. The tendency of exhibiting a cer-

tain level of plastic behavior has been generally observed on the cases studied, even in situations where the cross-section is classified as Class 4, as Figure 11 shows. Such results are especially responsible for the high R_{simul} ratios reported in Table 3.

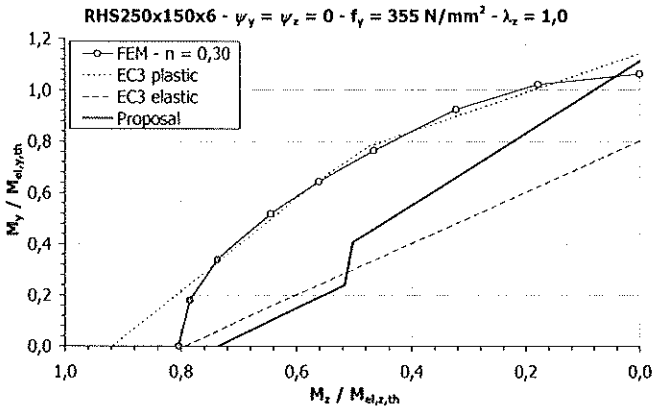

Figure 11. Situation where plastic reserve is observed while cross-section is Class 4 or nearly (first 3 points only are Class 4)

In addition to this "accuracy" parametric study, a second "safety" parametric study has been undertaken, aiming at the determination of so-called γ_{M1} safety factors. In this respect, some 576 additional cases have been studied, where all relevant geometrical and material data have been generated by random (using the Monte-Carlo simulation principles) and introduced in both the FEM models and the analytical calculations.

Table 4 gives further information on the statistical data used to generate the different parameters needed. A rigorous and strict application of EN 1990 Annex D (EN 1990 Annex D 2003) led to a $\gamma_{M1} = 1.03$ value, which complies with the recommended value of 1.10 in Eurocode 3.

Table 4. Statistical data for hollow specimens.

Parameter	Distribution	σ	V
h	Normal	1	0.005
b	Normal	1	0.01
t	Normal	1	0.05
f_y	Log-normal	1	0.06
$e_{loc.\ web}$	Normal	1	0.324
$e_{loc.\ flange}$	Normal	1	0.324
$e_{glob.\ y}$	Uniform	1	0.1
$e_{glob.\ z}$	Uniform	1	0.1

5 CONCLUSION

This paper has presented the essentials of a new design proposal for semi-compact hollow section beam-columns, that provides a fully continuous transition between Class 2 sections (i.e. exhibiting a plastic behavior) and Class 4 cross-sections (i.e. having an elastic resistance limited by effective properties).

Through extensive comparisons with both experimental tests and adequately-performed FEM simulation results, the new proposal was found accurate and safe. In addition, a safety factor $\gamma_{M1} = 1.03$ has been determined following the specifications of EN 1990, on the basis of FEM results obtained from another specific parametric study where all data have been generated by random; this γ_{M1} value complies with Eurocode 3 recommendations.

Whereas the new beam-column formulae have been incorporated in the latest version of Eurocode 3, the design proposal for Class 3 cross-sections results from recently achieved research projects, and is therefore not included in the Eurocode rules. Since the level of reliability of the model is found to be fully satisfactory, the model may be further proposed for implementation in the next draft of Eurocode 3.

6 ACKNOWLEDGEMENTS

The Research Fund for Coal and Steel (RFCS), by means of research project "Semi-Comp" n°RFS-CR-04044, as well as CIDECT, by means of research project 2X, are gratefully acknowledged.

7 REFERENCES

Austin, W.J. 1981. Strength and design of steel beam-columns. Proceedings of ASCE, *Journal of the Structural Division*, Vol. 87.

Boissonnade, N. Greiner, R. Jaspart, J.P. & Lindner, J. 2006. *Rules for Member Stability in EN 1993–1–1 – Background Documentation and Guidelines*, ECCS publication N 119.

Campus, F. & Massonnet, C. 1955. Recherches sur le flambement de colonnes en acier A37, à profil en double té, sollicitées obliquement. *Bulletin du CERES*, Liège, Tome VII.

CIDECT Research Project 2X, Jaspart, J.P. & Weynand, K. 2007. *Resistance and stability of structural members with hollow sections under combined compression and bending.*

CEN (Comité Européen de Normalisation) 1992. *Eurocode 3: Design of Steel Structures, Part 1–1: General Rules and Rules for Buildings (ENV 1993 1–1)*, Brussels.

CEN (Comité Européen de Normalisation) 2003. *EN 1990 Eurocode – Annex D. Basis of Design*, Brussels.

CEN (Comité Européen de Normalisation) 2005. *Eurocode 3: Design of Steel Structures, Part 1–1: General Rules and Rules for Buildings (EN 1993 1–1)*, Brussels.

Plastic member capacity of semi-compact steel sections – a more economic design ("Semi-Comp") 2007. Final report (01/01/05 – 30/06/07) – RFCS – Steel RTD (Contract RFS-CR-04044).